Tribology and Materials
Vol. 4, No. 4, 2025, pp. 220-232

ISSN 2812-9717
https://doi.org/10.46793/tribomat.2025.020

A TOPSIS multi-criteria evaluation of greases for wind turbine rolling bearings

Michal OKAL, Michal PROCHAZKA, Petr SVOBODA *, Ivan KŘUPKA, Martin HARTL

Faculty of Mechanical Engineering, Brno University of Technology, Brno, Czechia
*Corresponding author: petr.svoboda@vut.cz

Keywords

grease lubrication
rolling bearing
multi-criteria evaluation
TOPSIS method

History

Received: 12-08-2025
Revised: 31-10-2025
Accepted: 04-12-2025

Abstract

This work focuses on the use of the TOPSIS (technique for order of preference by similarity to ideal solution) multi-criteria evaluation methodology to assess the performance of greases intended for the main bearings of wind turbines. The goal was to design a testing system that enables a comprehensive evaluation of grease performance across key functional areas. The methodology evaluated four performance aspects: lubricating film formation, oil separation (grease bleeding), wear protection and frictional behaviour. Each test was designed with respect to the operating conditions of the main bearings and was experimentally validated. The results revealed differences in grease performance across the tests and confirmed the influence of varying test conditions. The collected data were analysed using the TOPSIS multi-criteria decision-making method, which enabled the integration of individual test results into a single comparative indicator. The method proved capable of comparing greases while maintaining result stability under varying weightings and input data. The final methodology provides a detailed framework for experimental testing and comprehensive performance evaluation of greases, offering a robust tool for their mutual comparison.

1. Introduction

Greases are semi-solid mixtures composed of base oil, thickener and additives, commonly used to lubricate bearings and other mechanical components. Their primary function is to separate contact surfaces, reduce friction and extend bearing life. Advantages include ease of application, sealing capability and corrosion protection. However, a key drawback is their limited service life, as grease degrades due to mechanical stress and thermal effects, which can lead to lubricant starvation. Therefore, regular relubrication is necessary, as defined by manufacturer-specified intervals [1].

When applying grease to the main bearing of a wind turbine, specific operating conditions must be considered – notably very low rotational speeds (10 – 15 rpm), irregular bearing motion, frequent start-stop cycles, wind turbulence and drivetrain dynamics [2]. To manage these conditions and compensate for misalignment, spherical or tapered roller bearings are typically used. Due to their line-contact geometry, these elements can withstand contact pressures up to 1.6 GPa under substantial loading conditions. [3]. The diameter of main bearings in wind turbines typically ranges from 300 to 600 mm in smaller machines (1 – 2 MW), while in modern large turbines (3 – 10+ MW) it commonly reaches 1,000 – 2,000 mm or more [2]. This work focuses on bearings with a diameter of approximately 500 mm, where at shaft speeds of 10 – 15 rpm the resulting contact velocity is about 0.25 – 0.5 m/s.

Grease lubrication in such bearings operates primarily in the elastohydrodynamic lubrication (EHL) regime. In EHL conditions, surfaces deform elastically, and the lubricant viscosity increases with pressure, allowing surface separation even at low speeds. Film thickness is influenced by viscosity, speed, load and by the geometry of contact

surfaces, their modulus of elasticity and lubricant piezo-viscous (pressure-viscosity) coefficient. The film thickness can be estimated using analytical models such as the Hamrock-Dowson equations [4]. At low speeds, thickener particles may enter the contact zone, temporarily increasing film thickness [5-7], although this effect cannot be predicted by standard equations. Thus, film formation depends not only on the base oil but also on the internal grease structure and its mechanical behaviour under low-speed conditions [8].

Due to low rotational speeds and frequent starts and stops, lubrication often occurs in the boundary regime, where the grease must not only form a film but also protect against wear. In this regime, additives play a crucial role. During operation, they may form protective boundary films on the surfaces, reducing friction and wear. Although extreme pressure (EP) and anti-wear (AW) additives are commonly used for low-speed, high-load applications, their influence on grease life remains poorly understood [9]. Many EP additives tend to bond with the polar thickener (e.g. metal soaps) rather than the metal surface, which may hinder their effectiveness. However, under very slow-motion conditions, the thickener structure may act as a carrier for the additives into the contact zone. Therefore, the performance of additives depends not only on their chemistry but also on the specific formulation of the grease and its response to mechanical and thermal ageing [10].

Grease degrades both mechanically and thermally. Mechanical shear disrupts the thickener structure, increasing oil separation and reducing film stability [8,11]. Thermal degradation leads to oxidation, although this is less critical in wind turbine main bearings, where temperatures rarely exceed 70 °C. Thus, mechanical degradation is considered the dominant failure mode [12].

Another important factor is friction, which in grease-lubricated bearings is determined not only by base oil viscosity but also by the interaction between the oil and the thickener. Studies show that greases often exhibit higher coefficients of friction than their base oils due to structural resistance in the contact zone [13]. At low sliding speeds, the thickener plays a key role in film formation, where its mechanical entrapment and deposition within the contact contribute significantly to the lubrication mechanism, even in rolling-sliding conditions [14]. In boundary and mixed lubrication regimes, wear is most critical, particularly during startup and shutdown when the lubricant film is not yet fully formed [15].

To evaluate grease performance across the mentioned properties, multiple tests are required. These tests differ in scale, units and optimisation goals, making single-parameter evaluation insufficient. To address this complexity, the TOPSIS method (technique for order of preference by similarity to ideal solution) provides a robust framework for ranking alternatives based on their geometric distance from an ideal and an anti-ideal solution [16,17]. It allows the simultaneous consideration of both beneficial and non-beneficial attributes without the need for complex pairwise comparisons or subjective scoring [18]. Thanks to its mathematical simplicity, transparency and proven applicability in tribological research, TOPSIS has become a widely accepted tool for evaluating lubricant performance under multi-criteria conditions [18-20].

The aim of this study is to perform a series of laboratory tests on commercially available greases designed for use in wind turbines. For comparison, one grease without a specific application focus was also tested. The results were subsequently evaluated using the TOPSIS method, enabling a comprehensive comparison of the tested greases. Based on this analysis, the most suitable grease was identified.

2. Experimental methods and materials

Four key performance properties of the greases: film thickness, oil separation (grease bleeding), wear resistance and friction, were evaluated through tribological testing. The tests were conducted under controlled laboratory conditions simulating the operating environment of wind turbine main bearings, including elevated temperature, moderate contact pressure and combined rolling/sliding motion.

2.1 Grease samples

Six commercially available greases were selected to provide a representative range of base oil viscosities, base oil types and thickener systems. Detailed properties of the tested samples are presented in Table 1. Samples G2 and G3 have the same composition but are from different manufacturers.

2.2 Film thickness measurement

The formation of the lubricating film was investigated using a ball-on-disc tribometer employing colourimetric interferometry, enabling

high-resolution film thickness measurements under EHL conditions. The device is briefly described here, and a detailed description is provided elsewhere [21]. The test specimens consisted of an AISI 52100 steel ball with a 25.4 mm diameter and a glass disc coated with a semi-transparent chromium layer to facilitate the precise detection of interference fringes generated by reflected white light. The load in the contact was applied by pressing the disc against the ball. To maintain fully flooded conditions, a grease wiper was attached to the underside to return the lubricant into the track. The configuration is shown in Figure 1. Measurements were performed at two nominal contact pressures (0.6 and 1.0 GPa) and two temperatures (25 and 50 °C), representing moderate and severe operating conditions typical of wind turbine main bearings. Entrainment speeds of 100, 200, 300, 400 and 500 mm/s were applied, with 300 mm/s selected as representative of typical operating conditions in wind turbine main bearings [22]. Discs made of optically smooth BK7 glass and sapphire were used, and all measurements were conducted under fully flooded lubrication conditions. Tests of samples under specific conditions were performed three times, and the results were averaged.

Table 1. Tested samples

Grease sample	Base oil kinematic viscosity at 40 °C, mm^2/s	Base oil type	Thickener type	Additive
G1	681	synthetic	lithium complex	EP and AW
G2	460	synthetic	lithium complex	EP and AW
G3	460	synthetic	lithium complex	EP and AW
G4	320	synthetic	lithium	EP and AW
G5	130	mineral	lithium complex	EP and AW
G6	130	mineral	lithium	no additives

2.3 Oil separation under static conditions

Oil separation was evaluated using a static separation method in accordance with DIN 51817, a standard procedure for assessing the oil retention capability of greases. A fixed amount of grease (30 g) was applied to a fine stainless-steel mesh placed over a collection vessel, and a

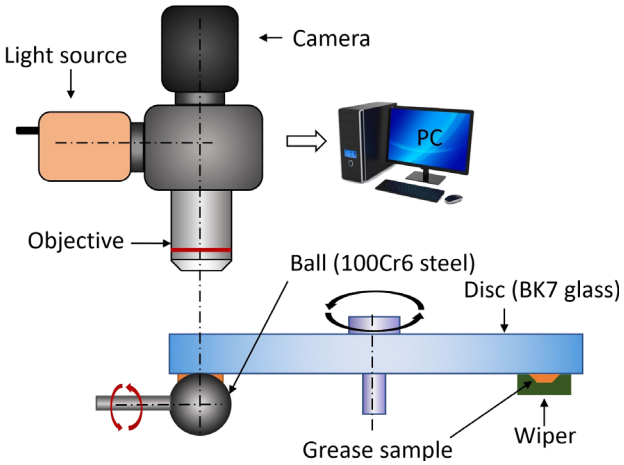

Figure 1. A schematic of the EHD rig used for film thickness measurement

constant load of 100 g was applied. The load was applied using dead weights, and the volume of oil released was measured. The set-up was exposed to 80 °C in a laboratory oven for 120 hours to simulate elevated thermal conditions typical of bearing environments. These test parameters were selected as mid-range values of the DIN 51817 standard to ensure both representativeness and sufficient severity. Fresh and mechanically degraded grease were compared.

Degradation was induced using a laboratory shear device constructed according to a previously published study [23], which subjected 30 g of grease to continuous shear for 24 hours, simulating thickener breakdown under prolonged mechanical stress in slow-speed bearings. The grease was subjected to shear stress in a 2 mm gap, with the internal drum rotating at 50 rpm. A more detailed description of the ageing process is provided by Zhou et al. [23].

After testing, the separated oil was weighed and expressed as a percentage of the original grease mass. The degradation-induced change in bleeding was quantified using the following relation:

$$\%\Delta = \left(\frac{m_d - m_f}{m_d} \right) 100, \quad (1)$$

where m_d is the mass of oil separated from the degraded sample and m_f is the mass separated from the fresh sample.

This value was later used as one of the decision criteria in the multi-criteria evaluation.

2.4 Wear measurement

The anti-wear performance of the lubricating greases was assessed using a ball-on-plate

configuration on a Bruker UMT TriboLab tribometer. The configuration is shown in Figure 2. The test employed reciprocating sliding with a 4 mm stroke under an applied normal load. A 7 mm diameter AISI 52100 steel ball served as the upper specimen, sliding against a flat AISI 52100 steel plate with a roughness of 0.1 µm to replicate conditions representative of mixed and boundary lubrication regimes. Wear scars formed on the plates were subsequently characterised using 3D optical profilometry to quantify material loss and surface damage.

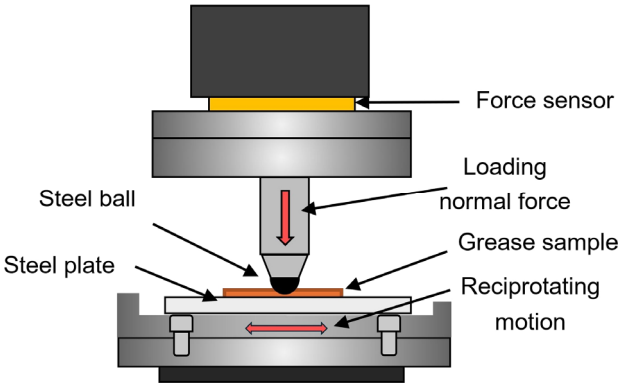

Figure 2. A schematic of the ball-on-plate rig used for wear measurement

The tests were conducted at a nominal contact pressure of 1.6 GPa to induce severe operating conditions. Two temperature settings were employed: ambient (room temperature) and elevated (80 °C). The low-temperature test duration was 3 minutes, while the high-temperature test was extended to 60 minutes to promote measurable wear scar formation. The average sliding speed was 0.25 m/s, and the total sliding distance covered during a single test was 570 m. Each test was repeated three times to ensure repeatability.

A controlled volume of lubricant (5 µl) was applied to the contact zone using a precision pipette. The wear volume, defined as the net material loss, was calculated and extrapolated over the entire stroke length. This value served as the primary quantitative metric for evaluating the grease's surface protection capability under adverse conditions. In the multi-criteria analysis, wear was treated as a cost criterion, with lower values indicating superior performance.

2.5 Friction measurement

The frictional behaviour of greases was investigated using a mini traction machine operating in a ball-on-disc configuration. The configuration is shown in Figure 3. This set-up allows independent control of ball and disc rotation, enabling precise definition of entrainment speed and slide-to-roll ratio (SRR). The objective was to characterise the transition from mixed to EHD lubrication regimes and assess the ability of the greases to maintain low friction under variable contact conditions. As a contact pair, a 19.05 mm ball was used with a disc (both made of AISI 52100 steel).

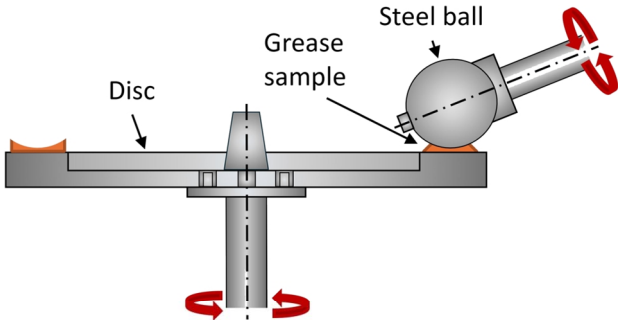

Figure 3. A schematic of the ball-on-disc rig used for friction measurement

Friction tests were conducted at a nominal Hertzian contact pressure of 1.0 GPa and a constant disc speed of 300 mm/s. The SRR varied in steps of 0, 2, 5 and 10 % to simulate increasing sliding intensity. Measurements were performed at two temperatures (25 and 50 °C) and with a 20 µl grease quantity. Before testing, all contact surfaces were cleaned with acetone and subjected to a 60-minute run-in procedure proposed by Galas et al. [24] to ensure repeatable contact geometry.

After cleaning, a defined volume of grease was applied to the contact zone in either a single- or double-droplet configuration. The coefficient of friction was measured continuously over 60-second intervals at each SRR level. Each test condition was repeated three times to assess repeatability, and average values were calculated. For TOPSIS evaluation, results at SRR = 2 % and SRR = 5 % at 50 °C were selected to represent typical operating conditions. Friction was treated as a cost criterion, where lower values indicate better energy efficiency and reliability.

2.6 TOPSIS method

To evaluate the overall performance of the grease across multiple tests, the TOPSIS was applied. This method allows for direct comparison of different results by ranking alternatives based on their distance from ideal and negative solutions. The application of the method is shown in Figure 4.

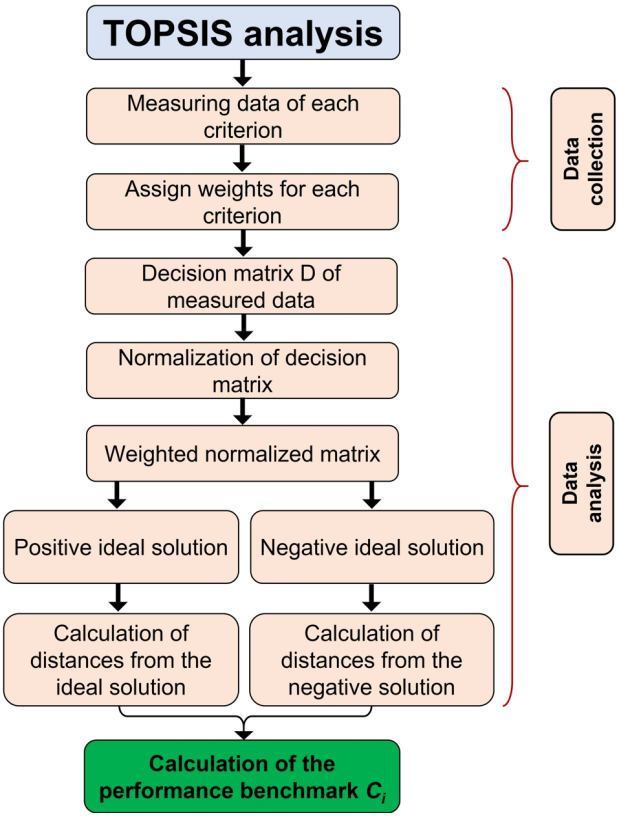

Figure 4. Schematic representation of the TOPSIS method

The following procedure was performed to evaluate the results of the tests on six greases.

Step 1: Decision matrix

$$D = [x_{ij}], \tag{2}$$

where x_{ij} represents the performance value of alternative i (grease sample) with respect to criterion j.

Two experimental variants, denoted as A and B, were defined to simulate representative and modified operating conditions of the main bearings of wind turbines. Variant A reflects typical thermal and mechanical loads, while variant B introduces altered measured parameters. The complete overview of both variants is summarised in Table 2.

Step 2: Normalised decision matrix

$$r_{ij} = \frac{x_{ij}}{\sqrt{\sum_{i=1}^{m} x_{ij}^2}}, \tag{3}$$

where r_{ij} is the normalised value of element x_{ij} for criterion j and m is the number of alternatives.

Step 3: Assign weights for each measured grease criterion. In the TOPSIS method, assigning appropriate weights w_j to individual criteria is a key step that directly affects the final ranking of alternatives. In this study, four different weighting strategies (W1 – W4) were applied to examine how prioritisation of different grease performance aspects influences the evaluation outcome.

Table 2. Summary of selected experimental conditions for both input datasets

Experiment	Variant A	Variant B
Film thickness	Hertzian stress 1 GPa speed 300 mm/s temperature 50 °C	Hertzian stress 1 GPa speed 300 mm/s temperature 25 °C
Bleeding change	30 g of grease on the mesh separation after 120 h at 80 °C	
Wear	Hertzian stress 1.6 GPa stroke 4 mm frequency 10 Hz temperature 80 °C	
Friction	Hertzian stress 1 GPa speed 300 mm/s temperature 25 °C 20 µl grease SRR 2 %	Hertzian stress 1 GPa speed 300 mm/s temperature 25 °C 20 µl grease SRR 5 %

W1 applied literature-based weighting. Based on recommendations from the literature [25], film thickness and grease bleeding stability are prioritised as critical properties for grease function under boundary conditions. Wear and friction are slightly lower, but still of relevant importance.

W2 applied performance-based weighting. This variant emphasises performance in demanding mixed lubrication regimes. Friction and wear are considered dominant, while film thickness and bleeding are treated as secondary properties that support contact separation.

W3 applied equal weighting. All four criteria are treated with equal importance, allowing unbiased comparison without prioritisation. This approach is often used as a neutral baseline.

W4 applied data variability-based weighting. This variant is derived from the stability of the experimental results. Criteria with lower standard deviations across all samples are assigned higher weights, under the assumption that more stable measurements provide more reliable input for decision-making.

To compute these weights, the inverse standard deviation approach was applied as follows:

$$\sigma_j = \sqrt{\frac{1}{n}\sum_{i=1}^{n}(r_{ij} - \bar{r}_j)^2}, \tag{4}$$

$$v_k = \frac{1}{\sigma_j}, \tag{5}$$

$$w_{jk} = \frac{v_k}{\sqrt{\sum_{k=1}^{m} v_k}}, \quad (6)$$

where σ_j is the standard deviation of criterion j, v_k is the unnormalised inverse variability and w_k is the normalised weight for criterion j.

The weights computed for all four variants are summarised in Table 3.

Table 3. Different applied weights

Weight	Film thickness	Bleeding change	Wear	Friction
W1, %	35	25	20	20
W2, %	25	20	30	25
W3, %	25	25	25	25
W4, %	22	14	13	51

Step 4: Weighted normalised matrix

$$v_{ij} = r_{ij} w_j, \quad (7)$$

where v_{ij} is the weighted normalised value, r_{ij} is the normalised value from Step 2 and w_j is the assigned weight for criterion j.

Step 5: Determination of ideal and negative solutions

$$A^+ = \{v_j^+\}, \quad (8)$$

$$A^- = \{v_j^-\}, \quad (9)$$

where v_j^+ is the best value for each criterion and v_j^- is the worst value for each criterion.

For the benefit criterion:

$$v_j^+ = \max(v_{ij}); \; v_j^- = \min(v_{ij}). \quad (10)$$

For the cost criterion:

$$v_j^+ = \min(v_{ij}); \; v_j^- = \max(v_{ij}). \quad (11)$$

Step 6: Determination of distance from ideal and negative solutions

$$S_i^+ = \sqrt{\sum_{j=1}^{m} (v_{ij} - v_j^+)^2}, \quad (12)$$

$$S_i^- = \sqrt{\sum_{j=1}^{m} (v_{ij} - v_j^-)^2}, \quad (13)$$

where S_i^+ is the Euclidean distance of alternative i from the ideal solution and S_i^- is the distance from the negative ideal solution.

Step 7: Relative closeness to the ideal solution

$$C_i = \frac{S_i^-}{S_i^+ + S_i^-}, \quad (14)$$

where C_i is the relative closeness of alternative i to the ideal solution. The alternative with the highest C_i is considered the best.

3. Results and discussion

3.1 Film thickness measurement

Figure 5 presents representative interferograms obtained at a rolling speed of 300 mm/s, contact pressure of 1 GPa and a temperature of 50 °C. In the case of samples G5 and G6, the thickener was more readily entrained into the contact zone, whereas for samples G1 – G4, the lubricating film predominantly consisted of base oil. The different colours of the areas correspond to different film thicknesses, as indicated in the legend. These visual patterns provide qualitative insight into the behaviour of grease in rolling contacts.

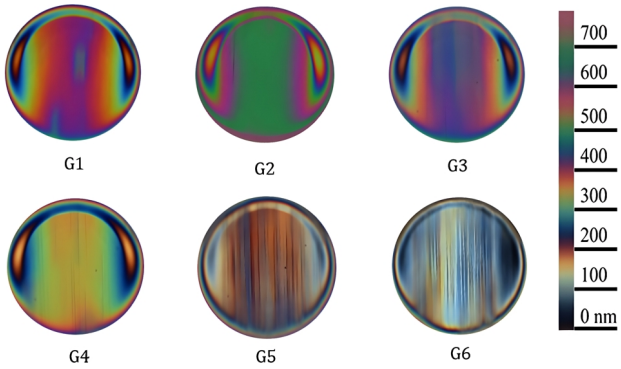

Figure 5. Interferograms of point contact at 300 mm/s, 50 °C and 1 GPa

Figure 6 highlights the differences in measurement results among the individual samples. At higher speeds, such as 300 mm/s, samples G1 – G4 exhibited good repeatability, whereas samples G5 and G6 showed greater variability, which can be attributed to the thickener entering the contact zone.

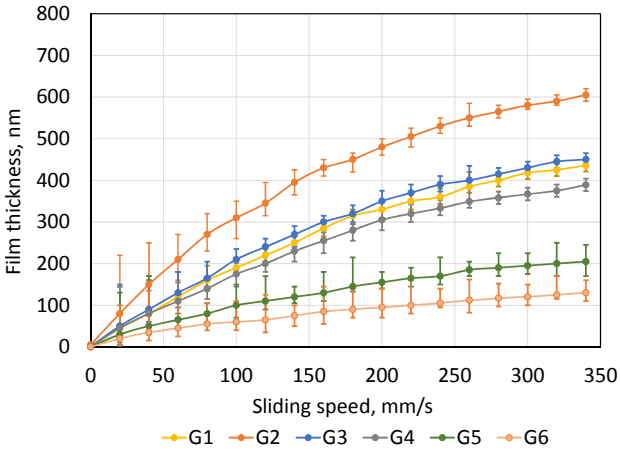

Figure 6. Film thickness at 50 °C and 1 GPa

Figure 7 illustrates the variations in average film thickness noticed at a rolling speed of 300 mm/s under different operating conditions. Although G1 contained the base oil with the highest viscosity, it did not achieve the greatest film thickness, suggesting that formulation synergy plays a more significant role. This notice is consistent with the findings of Gonçalves et al. [26] and Morales-Espejel et al. [27], who highlighted the critical influence of oil-thickener interactions on film stability under EHD conditions. For the multi-criteria evaluation, film thickness measured at 1.0 GPa and 50 °C was selected as a representative parameter and considered a benefit criterion. These values were chosen based on the normal operating conditions of the selected bearings.

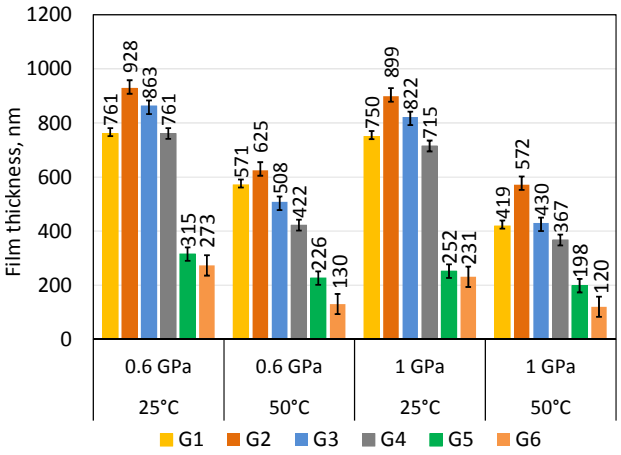

Figure 7. Average film thickness at 300 mm/s

3.2 Measurement of changes in bleeding properties

To assess the relative change in bleeding rate, the bleeding behaviour of fresh and mechanically degraded lubricant samples was compared, as shown in Figure 8. The results reveal notable differences in leakage stability among the tested lubricants. The slightest variation was noticed for G1 and G4, suggesting a high degree of structural integrity. In contrast, G5 exhibited the most pronounced increase in bleeding following mechanical degradation, indicating poor mechanical stability. Samples G2, G3 and G6 showed only minor changes.

These findings suggest that post-degradation stability is governed not only by base oil viscosity but also by the compatibility between the thickener network and the base oil. As highlighted by Lugt et. al. [28], maintaining structural integrity is essential for long-term oil retention. The robust performance of G1 and G4 reflects a well-balanced formulation capable of controlling bleeding even after exposure to shear. On the other hand, the marked instability of G5 points to a reduced oil-binding capacity under mechanical stress, which could compromise lubricant function during extended service intervals.

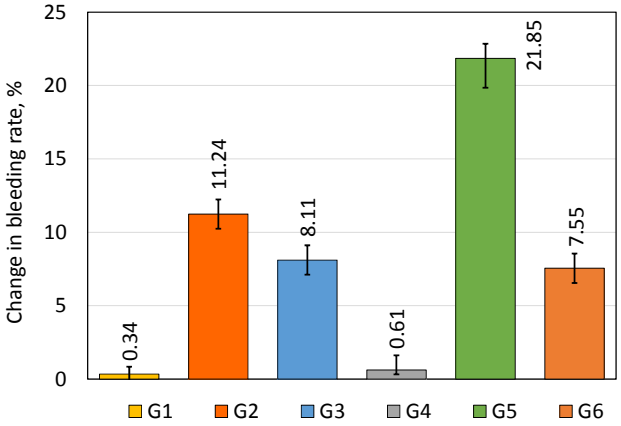

Figure 8. Average change in bleeding rate

3.3 Wear measurement

The tested lubricants were subjected to long-term wear testing with artificial heating to 80 °C. Figure 9 presents selected 3D surface profile images of wear scars obtained after testing, illustrating typical surface damage patterns associated with different lubricant compositions.

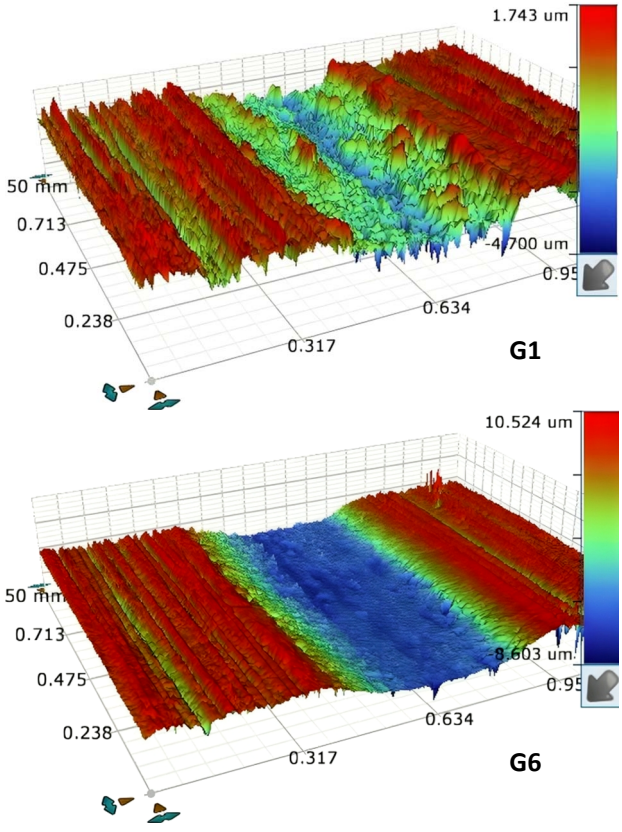

Figure 9. Example of steel plate wear with G1 and G6 grease

The corresponding steel plate worn volumes are summarised in Figure 10. Most lubricants exhibited excellent anti-wear performance, confirming the effectiveness of surface-protective additives. The lowest worn volumes were recorded for greases G2 and G5, indicating highly effective surface protection. In contrast, grease G6, which lacks EP additives, showed the highest wear. Although grease G4 contains additives, it exhibited relatively high wear due to its limited ability to form a stable lubricating film and the lower penetration capability of its thickener into the contact zone. These findings are consistent with previous studies by Peng et al. [25], who reported increased wear in the absence of protective additives and highlighted the role of thickener composition. Therefore, the wear test results at 80 °C were directly incorporated into the multi-criteria analysis.

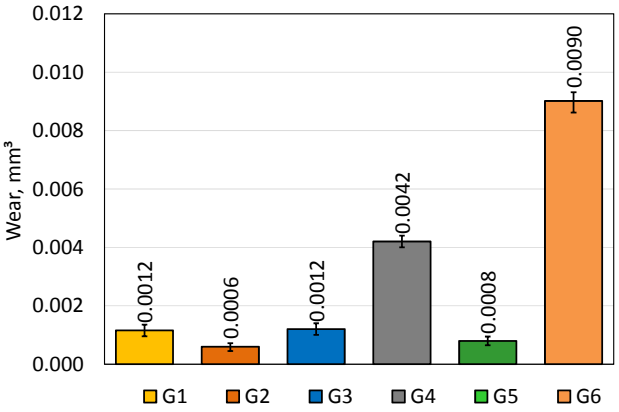

Figure 10. Average steel plate wear after testing

3.4 Friction measurement

Figures 11 and 12 present the coefficients of friction for all tested greases with SRR = 2 % and SRR = 5 %, respectively. These conditions were selected for further evaluation as they represent typical mixed lubrication regimes encountered in rolling bearings. The results clearly demonstrate that greases G1, G2 and G3 exhibited the lowest friction under both conditions. In contrast, grease G5 showed the highest friction at 5 % slip, suggesting traction-like behaviour. These findings confirm the significant influence of lubricant composition on frictional performance, consistent with previous studies by Wang and Wu [13]. Greases formulated with synthetic base oils and lithium complex thickeners (e.g. G1 and G3) consistently achieved lower friction levels, indicating a favourable structural balance.

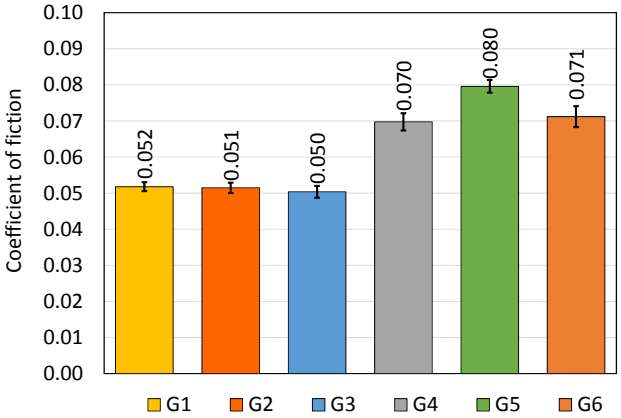

Figure 11. Coefficient of friction at an SRR of 2 %

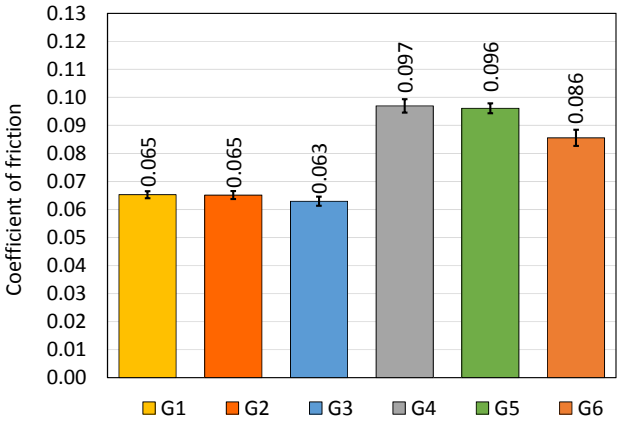

Figure 12. Coefficient of friction at an SRR of 5 %

3.5 Multi-criteria evaluation of results

Step 1: Decision matrix. Each grease variant was assigned a numerical value for each criterion, forming the initial decision matrix, as shown in Table 4. The criteria were classified into benefit or cost types based on their desired direction of optimisation.

Benefit criterion: Film thickness (larger-is-better), as thicker films improve surface separation, especially at extremely low speeds typical for wind turbine bearings [1,3].

Cost criterion: Bleeding change, wear and friction (smaller-is-better), as higher values are typically associated with structural instability, surface damage and increased coefficient of friction under mixed lubrication conditions common in wind turbine bearings [3,29,30].

This classification was necessary for subsequent steps in the TOPSIS method, especially when determining ideal and negative reference solutions.

Step 2: Normalised decision matrix. Values in the decision matrix were normalised using vector normalisation according to Equation (3). This step ensures comparability between criteria with different physical units. The values are shown in Table 5.

Table 4. Measured data in variant A

Grease sample	Film thick-ness, nm	Bleeding change, %	Wear, μm^3	Friction
G1	419	0.34	957,100	0.052
G2	580	11.24	544,100	0.052
G3	431	8.11	1,069,000	0.050
G4	343	0.61	4,521,000	0.069
G5	187	21.85	696,000	0.079
G6	113	7.55	8,762,000	0.071

Table 5. Normalised data of variant A

Grease sample	Film thick-ness, nm	Bleeding change, %	Wear	Friction
G1	0.451	0.013	0.097	0.333
G2	0.625	0.417	0.055	0.331
G3	0.464	0.301	0.108	0.324
G4	0.369	0.023	0.430	0.449
G5	0.201	0.810	0.070	0.512
G6	0.122	0.280	0.887	0.458

Step 3: Weighted normalised matrix. The weighted normalised matrix was computed by multiplying the normalised values from Step 2 by the weights assigned in Step 3, following Equation (7). This corresponds to the stage in Figure 4 and integrates both the performance and the importance of each criterion. Table 6 shows the results for the weighting strategy W1. The same procedure was repeated for W2, W3 and W4, but only W1 is presented due to space constraints.

Table 6. Weighted normalised data of variant A

Grease sample	Film thickness	Bleeding change	Wear	Friction
G1	0.158	0.003	0.019	0.067
G2	0.217	0.104	0.011	0.066
G3	0.162	0.075	0.022	0.065
G4	0.129	0.006	0.086	0.089
G5	0.070	0.203	0.014	0.103
G6	0.043	0.070	0.177	0.092

Step 4: Determination of ideal and negative solutions. The ideal (A^+) and negative ideal (A^-) solutions were determined based on the classification of each criterion, using Equations (8) to (11). Table 7 summarises the selected reference values.

Table 7. Ideal and negative solution values for variant A

Solution	Film thickness	Bleeding change	Wear	Friction
A^+	0.217	0.003	0.019	0.065
A^-	0.043	0.203	0.177	0.092

Step 5: Determination of distance from ideal and negative solutions. The Euclidean distance of each sample from the ideal and negative ideal solution was calculated using Equations (12) and (13). These distances quantify how closely each sample approaches the best or worst performance. The results are shown in Table 8.

Table 8. Ideal and negative solution values for variant A

Grease sample	S_i^+	S_i^-
G1	0.061	0.282
G2	0.101	0.264
G3	0.092	0.237
G4	0.119	0.234
G5	0.251	0.166
G6	0.253	0.133

Step 6: Relative closeness to the ideal solution. The final ranking was determined by calculating the relative closeness C_i of each sample to the ideal solution using Equation (14). This index combines both distances from Step 6 and reflects the overall performance. Results are shown in Figure 13.

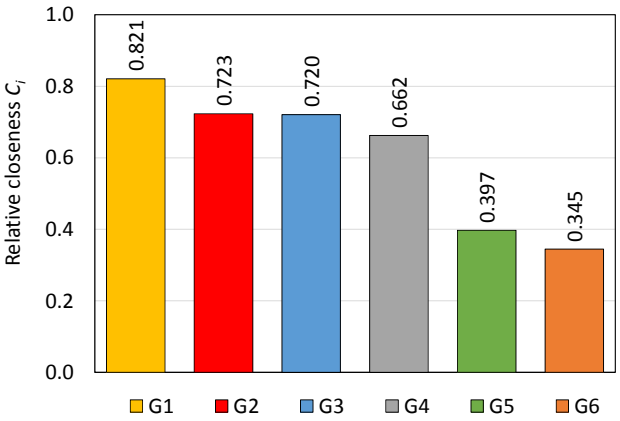

Figure 13. Relative closeness for variant A

The performance scores C_i, summarised in Figure 13, reveal that grease G1 achieved the highest closeness to the ideal solution, suggesting its favourable overall balance across all evaluated criteria under the W1 weighting strategy. Greases G2 and G3 followed closely, confirming their consistent performance in film thickness and friction. On the contrary, greases G5 and G6

received the lowest scores, reflecting their limited stability in bleeding and low film thickness. These results align with previous conclusions from individual tests and confirm the robustness of the TOPSIS framework for integrated grease evaluation.

3.6 Sensitivity analysis of weighing strategies

To assess how different weighting strategies affect the final ranking of greases, four strategies were compared: literature-based weights (W1), performance-based weights (W2), equal weights (W3) and data variability-based weights (W4). Each was applied to the same normalised matrix (Table 5) and processed using the TOPSIS method. Figure 14 compares the resulting C_i values, illustrating how prioritisation influences final performance scores.

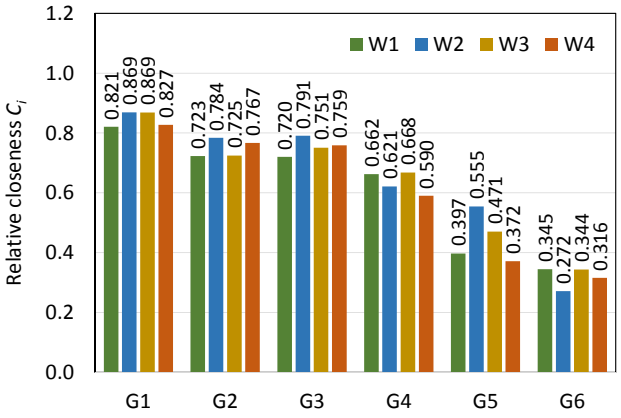

Figure 14. Relative closeness for different weights for variant A

Changes in the weighting strategy led to visible changes in the C_i performance index, particularly for mid-ranking greases. Grease G1 consistently achieved the highest score, reflecting stable performance in all weighting variants. On the contrary, grease G6 showed the most significant drop under W2, driven by poor wear and friction results, which were more prioritised. Equal weighting (W3) reduced these extremes, while data variability-based weighting (W4) highlighted greases with consistent experimental results. These trends confirm that inappropriate prioritisation can distort rankings, especially when test variability is high. As noted by Wang et al. [16] and Lee and Chang [17], weighting strategies that account for data stability improve reliability and confidence in decisions. Thus, the TOPSIS method proved sensitive to weighting inputs but capable of clearly distinguishing robust formulations when suitable strategies are applied.

3.7 Sensitivity analysis of data change

To evaluate the robustness and practical reliability of the proposed TOPSIS-based framework, the multi-criteria ranking was repeated using an alternative input dataset collected under different testing conditions (data from variant B). These conditions, previously detailed in Table 2, were selected to reflect plausible deviations from standard parameters, such as reduced temperature or modified heating protocols. By applying the same evaluation procedure and maintaining the original weighting strategy (W1), this analysis aimed to assess how sensitive the final grease rankings are to changes in the input of performance data.

The same evaluation procedure as in Section 3.5 was applied to dataset B (Table 9), using the W1 weighting strategy. The results shown in Figure 15 indicate that while the overall ranking remained relatively consistent, several greases exhibited significant changes in their C_i performance scores under the modified test conditions. In particular, greases G1 and G4 showed a significant increase in value, primarily due to greater film thickness formation at room temperature. The other greases maintained relatively stable positions, indicating better resistance to changes in test parameters.

Table 9. Measured data in variant B

Grease sample	Film thick-ness, nm	Bleeding change, %	Wear, μm^3	Friction
G1	745	0.34	957,100	0.065
G2	856	11.24	544,100	0.065
G3	807	8.11	1,069,000	0.063
G4	707	0.61	4,521,000	0.097
G5	259	21.85	696,000	0.096
G6	235	7.55	8,762,000	0.086

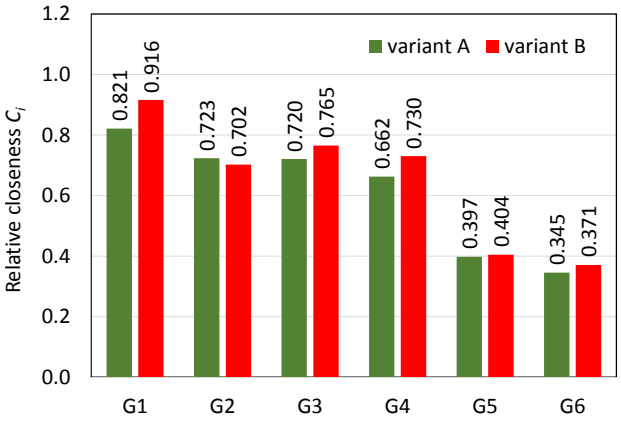

Figure 15. Relative closeness for variant A and variant B

These results indicate that the TOPSIS method successfully distinguishes greases with stable tribological behaviour from those more susceptible to operational changes. This aligns with the findings of Millek [31], who emphasised the influence of input conditions on performance variability and the need for robust evaluation schemes under realistic boundary conditions.

4. Conclusion

This study presents a tribological testing procedure combined with multi-criteria decision-making using the TOPSIS method for the systematic evaluation of the performance of greases used in the main bearings of wind turbines. It was noticed that multi-criteria evaluation can be effectively used to assess greases across several tests under different conditions and thus determine their suitability for a specific application.

It was confirmed that the thickness of the lubricating film is influenced not only by the viscosity of the base oil but also by the effect of the thickener. The interaction between these two components significantly affects changes in film thickness under varying temperature and pressure conditions.

The interaction between the thickener and base oil directly influences the grease's bleeding characteristics and mechanical stability. Moreover, it affects the thickener's ability to penetrate the contact zone, thereby reducing friction and wear.

The TOPSIS method demonstrated sensitivity to weighting inputs. However, minor adjustments to criterion weights did not alter the ranking of samples. Weighting strategies that account for data stability enhance the reliability of the results.

Changes in input test conditions had only a limited impact on the overall evaluation, confirming the ability of the TOPSIS method to identify greases with stable performance reliably.

The TOPSIS method enabled consistent evaluation of all tested parameters and clearly distinguished greases with superior performance across multiple tests. The applied evaluation approach correctly identified grease G6, which was not intended for the specified application, as the least suitable option.

This framework provides a reliable basis for the systematic evaluation of grease performance, taking into account multiple tribological properties. However, the tests were performed under laboratory conditions using simplified tribometers. Although these tests captured the basic performance characteristics of greases, further development of the methodology should include testing with real bearings under operating conditions.

Acknowledgement

This research work was supported by the Technology Agency of the Czech Republic (TACR), and it was co-financed by the National Competence Centre of Mechatronics and Smart Technologies under project number: TN02000010.

References

[1] P.M. Lugt, A review on grease lubrication in rolling bearings, Tribology Transactions, Vol. 52, No. 4, 2009, pp. 470-480, DOI: 10.1080/10402000802687940

[2] E. Hart, B. Clarke, G. Nicholas, A. Kazemi Amiri, J. Stirling, J. Carroll, R. Dwyer-Joyce, A. McDonald, H. Long, A review of wind turbine main bearings: Design, operation, modelling, damage mechanisms and fault detection, Wind Energy Science, Vol. 5, No. 1, 2020, pp. 105-124, DOI: 10.5194/wes-5-105-2020

[3] E. Hart, E. de Mello, R. Dwyer-Joyce, Wind turbine main-bearing lubrication – Part 1: An introductory review of elastohydrodynamic lubrication theory, Wind Energy Science, Vol. 7, No. 3, 2022, pp. 1021-1042, DOI: 10.5194/wes-7-1021-2022

[4] B.J. Hamrock, D. Dowson, Isothermal elastohydrodynamic lubrication of point contacts: Part 1 – Theoretical formulation, Journal of Lubrication Technology, Vol. 98, No. 2, 1976, pp. 223-228, DOI: 10.1115/1.3452801

[5] M. Okal, D. Kostal, J.A. Osara, P.M. Lugt, I. Krupka, M. Hartl, Experimental study of the effect of thickener on the film thickness in the contacts of a grease-lubricated ball bearing at low speed, Tribology Transactions, Vol. 68, No. 1, 2025, pp. 28-38, DOI: 10.1080/10402004.2024.2431523

[6] M. Okal, D. Kostal, K. Sakai, I. Krupka, M. Hartl, Thickener behaviour in rolling elastohydrodynamic lubrication contacts, Tribology Letters, Vol. 72, No. 3, 2024, Paper 72, DOI: 10.1007/s11249-024-01874-0

[7] M. Okal, D. Kostal, P. Sperka, I. Krupka, M. Hartl, Effect of contact conformity on grease lubrication, Lubricants, Vol. 10, No. 11, 2022, Paper 289, DOI: 10.3390/lubricants10110289

[8] H. Cen, P.M. Lugt, G. Morales-Espejel, Film thickness of mechanically worked lubricating grease at very low speeds, Tribology

Transactions, Vol. 57, No. 6, 2014, pp. 1066-1071, DOI: 10.1080/10402004.2014.933936

[9] A.G. Papay, Antiwear and extreme-pressure additives in lubricants, Lubrication Science, Vol. 10, No. 3, 1998, pp. 209-224, DOI: 10.1002/ls.3010100304

[10] H. Cen, N. de Laurentis, N. Bader, P.M. Lugt, Effect of thermal aging on the grease film thickness in ball bearings, Tribology International, Vol. 204, 2025, Paper 110511, DOI: 10.1016/j.triboint.2025.110511

[11] Y. Zhou, R. Bosman, P.M. Lugt, An experimental study on film thickness in a rolling bearing for fresh and mechanically aged lubricating greases, Tribology Transactions, Vol. 62, No. 4, 2019, pp. 557-566, DOI: 10.1080/10402004.2018.1539202

[12] P.M. Lugt, M. Holgerson, F. Reinholdsson, Impact of oxidation on grease life in rolling bearings, Tribology International, Vol. 188, 2023, Paper 108785, DOI: 10.1016/j.triboint.2023.108785

[13] Y. Wang, B. Wu, Friction characteristics and mechanisms of two lithium greases in elastohydrodynamic lubrication, Journal of Failure Analysis and Prevention, Vol. 20, No. 4, 2020, pp. 1266-1273, DOI: 10.1007/s11668-020-00932-8

[14] Y. Kanazawa, N. De Laurentis, A. Kadiric, Studies of friction in grease-lubricated rolling bearings using ball-on-disc and full bearing tests, Tribology Transactions, Vol. 63, No. 1, 2020, pp. 77-89, DOI: 10.1080/10402004.2019.1662147

[15] S. Wandel, N. Bader, F. Schwack, J. Glodowski, B. Lehnhardt, G. Poll, Starvation and relubrication mechanisms in grease lubricated oscillating bearings, Tribology International, Vol. 165, 2022, Paper 107276, DOI: 10.1016/j.triboint.2021.107276

[16] J.-J. Wang, Y.-Y. Jing, C.-F. Zhang, J.-H. Zhao, Review on multi-criteria decision analysis aid in sustainable energy decision-making, Renewable and Sustainable Energy Reviews, Vol. 13, No. 9, 2009, pp. 2263-2278, DOI: 10.1016/j.rser.2009.06.021

[17] H.-C. Lee, C.-T. Chang, Comparative analysis of MCDM methods for ranking renewable energy sources in Taiwan, Renewable and Sustainable Energy Reviews, Vol. 92, 2018, pp. 883-896, DOI: 10.1016/j.rser.2018.05.007

[18] H. Çalışkan, Selection of boron based tribological hard coatings using multi-criteria decision making methods, Materials & Design, Vol. 50, 2013, pp. 742-749, DOI: 10.1016/j.matdes.2013.03.059

[19] D.D. Trung, N.V. Thien, N.-T. Nguyen, Application of TOPSIS method in multi-objective optimization of the grinding process using segmented grinding wheel, Tribology in Industry, Vol. 43, No. 1, 2021, pp. 12-22, DOI: 10.24874/ti.998.11.20.12

[20] S. Opricovic, G.-H. Tzeng, Compromise solution by MCDM methods: A comparative analysis of VIKOR and TOPSIS, European Journal of Operational Research, Vol. 156, No. 2, 2004, pp. 445-455, DOI: 10.1016/S0377-2217(03)00020-1

[21] M. Hartl, I. Krupka, R. Poliscuk, M. Liska, J. Molimard, M. Querry, P. Vergne, Thin film colorimetric interferometry, Tribology Transactions, Vol. 44, No. 2, 2001, pp. 270-276, DOI: 10.1080/10402000108982458

[22] D.R. Lucas, K.K. Mistry, A tale of two greases: Comparison of wind energy grease performance using bench and component testing, Timken Technical Paper 36796.

[23] Y. Zhou, R. Bosman, P.M. Lugt, On the shear stability of dry and water-contaminated calcium sulfonate complex lubricating greases, Tribology Transactions, Vol. 62, No. 4, 2019, pp. 626-634, DOI: 10.1080/10402004.2019.1588445

[24] R. Galas, S. Skurka, M. Valena, D. Kvarda, M. Omasta, H. Ding, Q. Lin, W.-j. Wang, I. Krupka, M. Hartl, A benchmarking methodology for top-of-rail products, Tribology International, Vol. 189, 2023, Paper 108910, DOI: 10.1016/j.triboint.2023.108910

[25] H. Peng, H. Zhang, L. Shangguan, Y. Fan, Review of tribological failure analysis and lubrication technology research of wind power bearings, Polymers, Vol. 14, No. 15, 2022, Paper 3041, DOI: 10.3390/polym14153041

[26] D. Gonçalves, B. Graça, A.V. Campos, J. Seabra, J. Leckner, R. Westbroek, On the film thickness behaviour of polymer greases at low and high speeds, Tribology International, Vol. 90, 2015, pp. 435-444, DOI: 10.1016/j.triboint.2015.05.007

[27] G.E. Morales-Espejel, P.M. Lugt, H.R. Pasaribu, H. Cen, Film thickness in grease lubricated slow rotating rolling bearings, Tribology International, Vol. 74, 2014, pp. 7-19, DOI: 10.1016/j.triboint.2014.01.023

[28] P.M. Lugt, S. Velickov, J.H. Tripp, On the chaotic behavior of grease lubrication in rolling bearings, Tribology Transactions, Vol. 52, No. 5, 2009, pp. 581-590, DOI: 10.1080/10402000902825713

[29] E. Hart, E. de Mello, R. Dwyer-Joyce, Wind turbine main-bearing lubrication – Part 2: Simulation-based results for a double-row spherical roller main bearing in a 1.5 MW wind turbine, Wind Energy Science, Vol. 7, No. 4, 2022, pp. 1533-1550, DOI: 10.5194/wes-7-1533-2022

[30] J. Zhang, A. Wheatley, R. Pasaribu, E. Worthington, S. Matthews, C. Zinser, P. Cann, Wind turbine lubrication: Low temperature fretting wear

behaviour of four commercial greases, Tribology International, Vol. 187, 2023, Paper 108706, DOI: 10.1016/j.triboint.2023.108706

[31] J. Millek, The robustness of TOPSIS results using sensitivity analysis based on weight tuning, in L. Lhotska, L. Sukupova, I. Lacković, G. Ibbott (Eds.), World Congress on Medical Physics and Biomedical Engineering 2018, Vol. 2, Springer, Singapore, 2019, pp. 83-86, DOI: 10.1007/978-981-10-9038-7_15